Diffusion Barriers Block Defect Occupation on Reduced CeO$_2$(111)

P. G. Lustemberg,[1] Y. Pan,[2] B.-J. Shaw,[3] D. Grinter,[3] Chi Pang,[3] G. Thornton,[3] Rubén Pérez,[4]
M. V. Ganduglia-Pirovano,[5,*] and N. Nilius[6,†]

[1]*Instituto de Física Rosario (IFIR, CONICET-UNR) and Facultad de Ciencias Exactas,
Ingeniería y Agrimensura (UNR), 2000 Rosario, Argentina*
[2]*Institute of Physics, Chinese Academy of Sciences, P.O. Box 603, Beijing 100190, China*
[3]*Department of Chemistry and London Centre for Nanotechnology,
University College London, London WC1H 0AJ, United Kingdom*
[4]*Departamento de Fisica Teorica de la Materia Condensada and Condensed Matter Physics Center (IFIMAC),
Universidad Autonoma de Madrid, 28049 Madrid, Spain*
[5]*Instituto de Catálisis y Petroleoquímica (ICP-CSIC), 28049 Madrid, Spain*
[6]*Institute of Physics, Carl von Ossietzky University, 26111 Oldenburg, Germany*
(Received 31 March 2016; published 9 June 2016)

Surface defects are believed to govern the adsorption behavior of reducible oxides. We challenge this perception on the basis of a combined scanning-tunneling-microscopy and density-functional-theory study, addressing the Au adsorption on reduced CeO$_{2-x}$(111). Despite a clear thermodynamic preference for oxygen vacancies, individual Au atoms were found to bind mostly to regular surface sites. Even at an elevated temperature, aggregation at step edges and not decoration of defects turned out to be the main consequence of adatom diffusion. Our findings are explained with the polaronic nature of the Au-ceria system, which imprints a strong diabatic character onto the diffusive motion of adatoms. Diabatic barriers are generally higher than those in the adiabatic regime, especially if the hopping step couples to an electron transfer into the ad-gold. As the population of O vacancies always requires a charge exchange, defect decoration by Au atoms becomes kinetically hindered. Our study demonstrates that polaronic effects determine not only electron transport in reducible oxides but also the adsorption characteristics and therewith the surface chemistry.

Surface defects are of decisive importance for the physics and chemistry of oxides [1]. They represent local perturbations of the saturated metal-oxygen network and often comprise dangling-bond states and uncompensated surface charges. Not surprisingly, density-functional theory (DFT) finds defects to be the preferred adsorption sites for metal atoms and molecules on oxide surfaces [2,3], with oxygen vacancies being the most relevant type due to their relatively low formation energy [4,5]. On nonreducible MgO, for example, Au atoms substantially bind to O defects, while the ideal surface offers weak van der Waals interactions only [6]. The same holds for ceria, as a reducible oxide [7–9]. Again, gold hardly interacts with the stoichiometric surface, while binding to surface O vacancies ($V_O{}^S$) is highly favorable and accompanied by an electron transfer from a nearby Ce^{3+} ion [10]. Defects are also involved in stabilizing and activating molecular species and therefore of relevance for oxide chemistry [11].

While theory suggests a large impact of defects on various oxide properties, the correlation is not so clear on the experimental side. Predominantly defect-mediated adsorption is found for weakly bound adsorbates, e.g., for water and methanol on TiO$_2$(110) [12,13] and V_2O$_3$(0001) [14]. For more reactive species, such as metals, the interplay between adsorption and surface

defects is less obvious. According to STM data, the binding of metal atoms to thin MgO [15] and alumina films [16] is hardly affected by point defects. For Au/V_2O$_3$(0001) [17] and Cu/CeO$_2$(111) [18], even the hindered occupation of defects was reported. Also, nonlocal spectroscopic techniques failed to prove the relevance of defects in certain adsorption processes. Photoemission studies of reduced CeO$_2$ and Fe$_3$O$_4$ sparsely loaded with gold detected mainly cationic Au species [19,20], although binding to O vacancies should result in negatively charged atoms [5,7,9]. Similarly, cationic gold and not Au$^-$ species associated with O vacancies were observed on defective MgO [21]. Finally, the yield of ceria-catalyzed water-gas-shift reactions was found to be unchanged after removing neutral and anionic noble-metal clusters, leaving only cationic species that typically bind to the stoichiometric surface as active elements [22].

In this Letter, we address the discrepancy between the anticipated importance of O defects for the adsorption on oxide surfaces and the actual role derived from experiment. For this purpose, we examine the temperature-dependent binding behavior of Au atoms on CeO$_{2-x}$(111) films, using a combination of STM and DFT. We find only a small number of adatoms attached to $V_O{}^S$ defects, despite a clear binding preference predicted by theory. We explain this

result with diffusion barriers around the V_O^S sites that cannot be overcome by Au atoms at moderate temperature. Our study thus gives insight into the kinetics of defect population on oxide surfaces and elucidates why a purely thermodynamic picture sometimes deviates from the experimental findings.

The experiments were performed in two ultrahigh-vacuum STM setups operated at 5 and 300 K. Ceria films of 3–5 trilayer thickness were grown at room temperature by reactive Ce deposition in 5×10^{-6} mbar O_2 either on Ru(0001) or Pt(111) crystals [23,24]. A V_O^S-defect concentation of ~5×10^{13} cm^{-2} was adjusted by annealing the films in vacuum to 1000 K [Fig. 1(a)]. The vacancies show up in the STM as circular depressions or double and triple protrusions at negative and positive sample bias, respectively [Figs. 1(b) and 1(c)] [25]. Individual Au atoms were dosed from a thermal evaporator at either 15 or 300 K onto the Ru- and Pt-supported films. The samples were equilibrated afterwards by annealing them to a desired temperature between 50 and 400 K.

Spin-polarized DFT + U calculations were carried out with the Dudarev approach ($U - J = 4.5$ eV) [26] and the Perdew-Burke-Ernzerhof exchange-correlation functional as implemented in VASP [27,28]. The Ce ($4f$, $5s$, $5p$, $5d$, $6s$), O ($2s$, $2p$), and Au ($6s$, $5d$) electrons were explicitly treated as valence states, expanded into plane waves with 400 eV energy cutoff. The remaining electrons were described with the projector-augmented wave method [29]. $CeO_2(111)$ slabs were modeled by two O-Ce-O trilayers with a (3×3) surface cell, separated by ~10 Å of vacuum. While the bottom trilayer was fixed at bulk positions, the other atoms were allowed to relax. Electronic properties were calculated with a $2 \times 2 \times 1$ Monkhorst-Pack k-point mesh. The presence of the metal substrate was neglected, as it imposes only minor lattice distortions onto the ceria film. Moreover, experimental films were too thick to enable direct electron exchange between adsorbates and the metal support. The climbing-image nudged elastic-band method [30] was used to locate

transition states and energy barriers along gold diffusion paths across the surface [31].

Figure 1(d) depicts a typical CeO_{2-x} region after Au deposition. The appearance of Au atoms depends on their position on either regular or defect sites in the surface [Fig. 2(a)] [32]. Atoms trapped by a V_O^S hardly protrude off the surface and are surrounded by three dents pointing to the symmetry directions of the ceria lattice. In contrast, regularly bound Au shows up as 2-Å-high feature at +2.5 V sample bias. While gold gets easily displaced on the stoichiometric surface during scanning, adatoms bound to O defects do not move under influence of the tip. A distinction between regular and defect-bound species is difficult for larger aggregates that appear with variable height depending on their atom count [33].

An identical CeO_{2-x} region before and after Au exposure is displayed in Figs. 2(b) and 2(c). The V_O^S sites are distinguishable as clear depressions; the Au atoms and their binding sites before adsorption are marked by circles. Apparently, none of the five adatoms has reached one of the numerous defects. Instead, threefold Ce hollows are identified as binding sites that are, however, indistinguishable from adjacent O-O bridge positions at the resolution of STM. Note that the latter are the preferred Au binding sites according to DFT [34].

The temperature-dependent Au diffusion behavior was examined in a subsequent experiment [Figs. 2(d)–2(f)]. For this purpose, gold was dosed onto the surface at 15 K and annealed afterwards to a given temperature. Directly after exposure, single adatoms and V_O^S defects were the dominant surface species and the peculiar fingerprint of Au@V_O^S complexes was hardly found [Fig. 2(d), inset]. Statistical evaluation yields that only one out of 25 atoms actually sits in a V_O^S site upon 15 K deposition. To explore whether this small number relates to the finite mobility of Au atoms at a low temperature, the samples were annealed to 200 K and subsequently imaged at 5 K [Fig. 2(e)]. Still, a negligible number of Au atoms were found to bind to V_O^S defects, although the presence of Au aggregates clearly
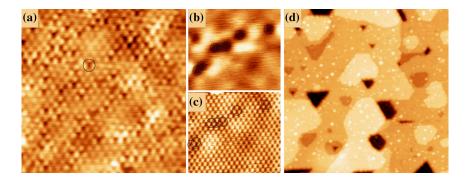

FIG. 1.   (a) Atomically resolved STM image of CeO_{2-x}/Ru(0001), showing V_O^S defects as depressions (−1.7 V, 25 pA, 10×10 nm^2). (b) Filled (−2.5 V) and (c) associated empty-state image (+1.7 V) of several V_O^S marked by black circles (6×5 nm^2). While the vacancies are clearly visible at negative bias, mainly the Ce^{4+} ions in the surface are detected at positive polarity. (d) Overview STM image taken after 0.05 ML Au deposition at 5 K (2.5 V, 100×100 nm^2).
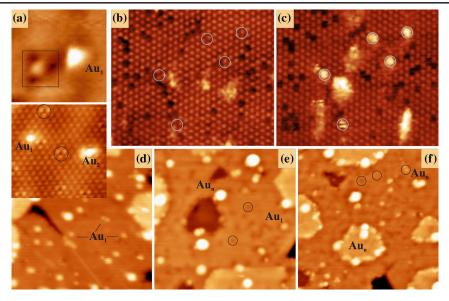
FIG. 2. (a) High-resolution STM image of a regular and a defect-bound Au atom (box) on $CeO_{2-x}/Ru(0001)$ ($+2.5$ V, 3.8×3.0 nm^2). (b),(c) Identical surface region on a $\sqrt{3}$-reconstructed $CeO_{2-x}/Pt(111)$ film before and after exposure of 0.05 ML Au (-3.0 V, 10.5×8.0 nm^2). Adatoms and their binding sites on the pristine surface are marked by circles. (d) $CeO_{2-x}/Ru(0001)$ after gold deposition at 15 K and (e) after annealing to 200 and (f) 400 K (2.5 V, 30×30 nm^2). The inset in (d) shows a close-up of the main image; some $V_O{}^S$ defects are encircled.

marked the onset of diffusion. After 400 K annealing, gold mostly appeared in the form of clusters along the oxide step edges, while undecorated $V_O{}^S$ defects remained visible with high density ($\sim 5 \times 10^{13}$ cm^{-2}). An upper bound of defects that have actually trapped an Au atom is obtained from the number of clusters located away from step edges within the oxide terraces [2.5×10^{12} cm^{-2}, Fig. 2(f)].

Our STM measurements therefore suggest that $V_O{}^S$ defects in $CeO_{2-x}(111)$ are unable to attract Au atoms in large numbers. This conclusion is supported by a statistical data evaluation that finds a similar probability for an Au atom to land on an arbitrary surface site and for observing an atom in a $V_O{}^S$ defect (Table I). Apparently, the vacancies do not trap gold even if diffusion is permitted, and only those atoms that land directly on a $V_O{}^S$ do bind. A plausible explanation would be the presence of diffusion barriers that prevent the Au atoms from reaching the $V_O{}^S$ defects, an assumption that will be tested by DFT calculations next.

TABLE I. Statistical evaluation of the density of Au atoms and $V_O{}^S$ sites on $CeO_{2-x}(111)$. Note the similar ratio between Au atoms and regular O sites compared to Au atoms trapped by $V_O{}^S$ defects.

Species	Density [nm^{-2}]	Ratio
Surface oxygen	7.91	Au/surface oxygen: 1.5%
Au atoms	0.12 ± 0.04	
$V_O{}^S$ sites	0.47 ± 0.05	Au@$V_O{}^S$/$V_O{}^S$ sites: 1.1%
Au@$V_O{}^S$ sites	0.005 ± 0.002	

To evaluate the role of kinetic effects, the Au binding energy on stoichiometric and defective ceria has been calculated first. In agreement with the literature [7,8,34], O bridge sites are energetically preferred on the ideal surface (-1.05 eV), while binding to a $V_O{}^S$ is considerably stronger (-2.37 eV) [31]. On stoichiometric ceria, gold forms a cation (Au$^+$) by donating an electron to a nearby Ce^{4+} ion. It becomes neutral (Au^0) within the first coordination shell of a $V_O{}^S$ defect and turns into an anion after defect population via charge transfer from a Ce^{3+} ion. This electron exchange substantially stabilizes the binding configuration and makes $V_O{}^S$ the favorable Au adsorption site, in conflict with the experimental data. To move beyond a static adsorption picture, we have addressed kinetic effects by calculating energy barriers that occur during atom diffusion into the vacancies. Adatom motion in general may follow an adiabatic or diabatic regime. In the former, structural relaxation of the oxide lattice and electron exchange with the ad-gold is enabled at each diffusion step, while both effects are prohibited in the latter. Adiabatic diffusion reliably describes experimental situations in which either the diffusing species causes little surface distortion or structural relaxations are fast with respect to adatom hopping. Both conditions are not fulfilled here, as the Au atom substantially distorts the ceria lattice and produces a polaronic state [35].

We start our analysis by evaluating the adiabatic diffusion landscape on stoichiometric ceria. A typical path of an Au$^+$ ion runs from a stable O bridge to adjacent hollow and top sites (Fig. 3); other paths are given in Ref. [31]. The associated potential barriers are generally low and reach a
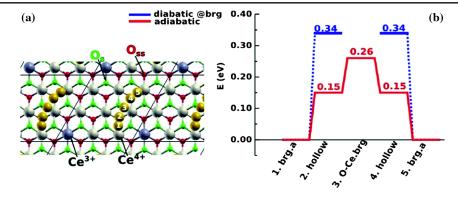
FIG. 3.   (a) Au-diffusion path on stoichiometric $CeO_2(111)$. (b) Adiabatic (red line) and diabatic (blue line) barriers for an Au^+ species moving along the depicted path. For the diabatic calculation, the surface was frozen in the equilibrium configuration for the O bridge (brg.a) site.

maximum of 0.29 eV. In presence of a $V_O{}^S$, the barrier depends on the selected path into the vacancy, the position of the Ce^{3+} ions, and the Au charge state but lies again in between 0.2 and 0.3 eV (Fig. 4). The transition state locates in the second coordination shell of the $V_O{}^S$, and the associated barrier relates to the defect-induced lattice distortion, i.e. to the outward relaxation of adjacent Ce^{4+} ions, the upward movement of second-neighbor O^{2-}, and the extra space required by the Ce^{3+} ion pair [36]. Further contributions come from the variable Au charge state that evolves from +1 (repulsive with respect to $V_O{}^S$) to 0 and −1 upon approaching the defect. Note that the diffusion potential bears striking similarities to Ehrlich-Schwöbel barriers that govern adsorbate motion across step edges on metallic and dielectric surfaces [37]. Using transition

state theory, the adiabatic barrier of ∼0.3 eV can be transformed into a temperature onset for diffusion, defined as the temperature at which the hopping rate reaches 1 Hz. With an exponential prefactor of 1.7×10^{13} Hz, matching the longitudinal optical (LO) phonon of ceria, adatom diffusion is expected to start at 115 K on the stoichiometric and defective surface. As no $V_O{}^S$ decoration is observed even at 300 K, the adiabatic picture seems, however, inappropriate to describe diffusion processes on $CeO_{2-x}(111)$.

To model Au diffusion in the diabatic limit, the ceria lattice was frozen and the Au charge state fixed along the path of motion. Two energetically favorable O bridge sites, both binding gold as a cation, were selected as starting positions (Fig. 4). This procedure reproduces our experiments, in which Au was dosed at a low temperature and
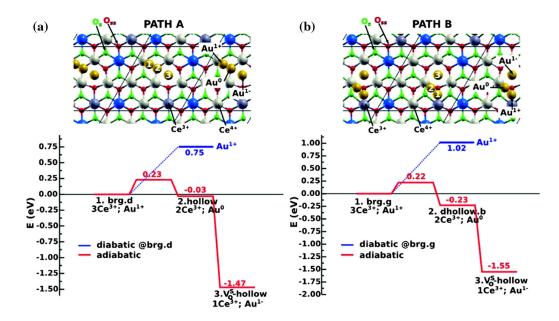

FIG. 4.   Nonstoichiometric surface: Adiabatic (red line) and diabatic (blue line) diffusion barriers for an Au atom moving along two different pathways into a O vacancy (position no. 3). For the diabatic calculations, the surface was frozen in the equilibrium configuration of an Au atom in two different bridge sites. Ce^{3+} ions that keep their $4f$ electron as the Au moves are depicted in dark gray, while ions involved in the Au charge transfer are blue.

diffusion was initiated via annealing. In the diabatic regime, an increasing mismatch between the fixed Au charge state on the frozen lattice and the relaxed solution develops, and the total energy of the system increases quadratically along the path [35]. The respective barrier heights are up to 3 times larger than in the adiabatic case ($\sim$1.0 eV). Translated into a temperature, diffusive motion into the O vacancies may thus be expected only above 395 K, explaining why defect occupation is impossible at room temperature. Interestingly, diabatic barriers are clearly lower on the stoichiometric surface, where the Au charge state is +1 on all sites. Here, diffusion paths with $\sim$0.3 eV activation energy prevail, explaining the observed aggregation of gold already at 300 K. In a nutshell, the blocked decoration of $V_O{}^S$ sites seems to arise from large diabatic barriers induced by changes of the Au charge state upon approaching a defect.

Changing charge configurations in the adiabatic regime imply that the diffusing adatom probes potential energy surfaces (PESs) that belong to different charge states. Conversely, the system proceeds along a single PES in the diabatic limit, where surface structure and Au charge are frozen along the path. A realistic diffusion path from an initial to a final position $a \rightarrow b$ now includes transitions between the different PESs. The transition probability P_{ab} can be estimated with the Landau-Zener formula [35]:

$$P_{ab} = 1 - \exp\left[\frac{-V_{ab}^2}{h\nu}\sqrt{\frac{\pi^3}{\lambda \times kT}}\right]. \qquad (1)$$

Here, v is the driving phonon frequency that corresponds to the LO phonon of ceria, and λ is the reorganization energy of the system, i.e., the excess energy of a diffusing species at site b but with the charge and relaxation state matching the initial a position. The key parameter for a predominantly diabatic or adiabatic nature of the process is, however, the matrix element V_{ab} that accounts for the electronic coupling of the two states. Whereas strong coupling leads to $P_{ab} \rightarrow 1$ (adiabatic diffusion), diabatic motion prevails at small V_{ab} ($P_{ab} \rightarrow 0$). Bulk calculations for reducible oxides demonstrated that the magnitude of V_{ab} largely depends on the distance between the two centers exchanging electrons [38]. For rutile TiO$_2$, a V_{ab} of 200 meV has been calculated for polaron hopping between two [001]-oriented Ti sites spaced by 2.97 Å [38]. This value reduces to 10 meV along the [111] direction, where the Ti atoms are 3.61 Å apart. For bulk ceria with 3.80 Å Ce—Ce distance, a V_{ab} of 65 meV was calculated, still polaron hopping follows the adiabatic regime [35]. In our case, the charge exchange between a diffusing Au$^+$ and a nearby Ce^{3+} ion occurs at much larger distances, e.g., at 4.7 $-$4.8 Å for the paths in Fig. 4. The corresponding matrix element is thus expected to be smaller than in bulk ceria, imprinting a strong diabatic nature onto the diffusive motion. Note that the adiabatic character increases with

decreasing temperature due to the smaller denominator in the exponential term of Eq. (1). However, the attempt frequency controlled by an Arrhenius term drops as well, and defect decoration thus remains impossible despite much lower barriers than in the diabatic regime.

In conclusion, Au adsorption on CeO$_{2-x}$(111) is largely governed by kinetic aspects that prohibit occupation of the thermodynamically preferred $V_O{}^S$ defects. In fact gold diffusion into O vacancies follows a diabatic path due to the need of the adatom to exchange electrons with nearby Ce^{3+} ions. On the stoichiometric surface, the Au atom keeps a constant +1 charge, and potential barriers, in both the adiabatic and diabatic limit, are small. Our study illustrates the complexity of diffusion phenomena that are coupled to polaronic lattice distortions and charge-transfer processes. This interplay results in a kinetically controlled adsorption behavior that deviates from pure thermodynamics and in which surface defects play a minor role. Especially the latter fact may change our perception of the importance of surface defects for the physics and chemistry of reducible oxides.

P. G. L. and Y. P. contributed equally to this work.

*Corresponding authors.
 vpg@icp.csic.es
†niklas.nilius@uni-oldenburg.de

[1] V. E. Henrich and P. A. Cox, The Surface Science of Metal Oxides (Cambridge University Press, Cambridge, England, 1996).
[2] A. V. Matveev, K. M. Neyman, I. V. Yudanov, and N. Rosch, Surf. Sci. **426**, 123 (1999).
[3] M. V. Ganduglia-Pirovano, A. Hofmann, and J. Sauer, Surf. Sci. Rep. **62**, 219 (2007).
[4] G. Pacchioni, Chem. Phys. Chem. **4**, 1041 (2003).
[5] J. Paier, C. Penschke, and J. Sauer, Chem. Rev. **113**, 3949 (2013).
[6] A. Del Vitto, G. Pacchioni, F. O. Delbecq, and P. Sautet, J. Phys. Chem. B **109**, 8040 (2005).
[7] Y. Chen, P. Hu, M.-H. Lee, and H. Wang, Surf. Sci. **602**, 1736 (2008).

[8] C. Zhang, A. Michaelides, and S. J. Jenkins, Phys. Chem. Chem. Phys. **13**, 22 (2011).

[9] M. M. Branda, N. J. Castellani, R. Grau-Crespo, N. H. de Leeuw, N. C. Hernandez, J. F. Sanz, K. M. Neyman, and F. Illas, J. Chem. Phys. **131**, 094702 (2009).

[10] N. C. Hernández, R. Grau-Crespo, N. H. de Leeuw, and J. F. Sanz, Phys. Chem. Chem. Phys. **11**, 5246 (2009).

[11] M. F. Camellone and S. Fabris, J. Am. Chem. Soc. **131**, 10473 (2009).

[12] O. Bikondoa, C. L. Pang, R. Ithnin, C. A. Muryn, H. Onishi, and G. Thornton, Nat. Mater. **5**, 189 (2006).

[13] Z. R. Zhang, O. Bondarchuk, J. M. White, B. D. Kay, and Z. Dohnalek, J. Am. Chem. Soc. **128**, 4198 (2006).

[14] D. Gobke, Y. Romanyshyn, S. Guimond, J. M. Sturm, H. Kuhlenbeck, J. Dobler, U. Reinhardt, M. V. Ganduglia-Pirovano, J. Sauer, and H. J. Freund, *Ang. Chem., Int. Ed.* 48, 3695 (2009).

[15] M. Sterrer, T. Risse, U. M. Pozzoni, L. Giordano, M. Heyde, H.-P. Rust, G. Pacchioni, and H.-J. Freund, Phys. Rev. Lett. **98**, 096107 (2007).

[16] N. Nilius, M. V. Ganduglia-Pirovano, V. Brázdová, M. Kulawik, J. Sauer, and H.-J. Freund, Phys. Rev. Lett. **100**, 096802 (2008).

[17] N. Nilius, M. V. Ganduglia-Pirovano, M. V. Brázdová, V. Simic-Milosevic, J. Sauer, and H.-J. Freund, New J. Phys. **11**, 093007 (2009).

[18] T. E. James, S. L. Hemmingson, and C. T. Campbell, ACS Catal. **5**, 5673 (2015).

[19] M. Baron, O. Bondarchuk, D. Stacchiola, S. Shaikhutdinov, and H. J. Freund, J. Phys. Chem. C **113**, 6042 (2009).

[20] K. T. Rim, D. Eom, L. Liu, E. Stolyarova, J. M. Raitano, S.-W. Chan, M. Flytzani-Stephanopoulos, and G. W. Flynn, J. Phys. Chem. C **113**, 10198 (2009).

[21] M. A. Brown, F. Ringleb, Y. Fujimori, M. Sterrer, H. J. Freund, G. Preda, and G. Pacchioni, J. Phys. Chem. C **115**, 10114 (2011).

[22] Q. Fu, H. Saltsburg, and M. Flytzani-Stephanopoulos, Science **301**, 935 (2003).

[23] D. R. Mullins, P. V. Radulovic, and S. H. Overbury, Surf. Sci. **429**, 186 (1999).

[24] D. R. Mullins, L. Kundakovic, and S. H. Overbury, J. Catal. **195**, 169 (2000).

[25] J.-F. Jerratsch, X. Shao, N. Nilius, H.-J. Freund, C. Popa, M. V. Ganduglia-Pirovano, A. M. Burow, and J. Sauer, Phys. Rev. Lett. **106**, 246801 (2011).

[26] S. L. Dudarev, G. A. Botton, S. Y. Savrasov, C. J. Humphreys, and A. P. Sutton, Phys. Rev. B **57**, 1505 (1998).

[27] J. P. Perdew, K. Burke, and M. Ernzerhof, Phys. Rev. Lett. **77**, 3865 (1996).

[28] G. Kresse and J. Haffner, Phys. Rev. B **49**, 14251 (1994); G. Kresse and J. Furthmüller, Phys. Rev. B **54**, 11169 (1996).

[29] P. E. Blöchl, Phys. Rev. B **50**, 17953 (1994); G. Kresse and D. Joubert, Phys. Rev. B **59**, 1758 (1999).

[30] G. Henkelman and H. Jónsson, J. Chem. Phys. **113**, 9901 (2000).

[31] See Supplemental Material at http://link.aps.org/supplemental/10.1103/PhysRevLett.116.236101 for Au adsorption configurations, adiabatic and diabatic diffusion pathways.

[32] Y. Pan, N. Nilius, H.-J. Freund, J. Paier, C. Penschke, and J. Sauer, Phys. Rev. Lett. **111**, 206101 (2013).

[33] Y. Pan, Y. Cui, C. Stiehler, N. Nilius, and H.-J. Freund, J. Phys. Chem. C **117**, 21879 (2013).

[34] K. Kósmider, V. Brázdová, M. V. Ganduglia-Pirovano, and R. Pérez, J. Phys. Chem. C **120**, 927 (2016).

[35] J. J. Plata, A. M. Márquez, and J. F. Sanz, J. Phys. Chem. C **117**, 14502 (2013).

[36] M. V. Ganduglia-Pirovano, J. L. F. Da Silva, and J. Sauer, Phys. Rev. Lett. **102**, 026101 (2009).

[37] G. Ehrlich and F. G. Hudda, J. Chem. Phys. **44**, 1039 (1966); R. L. Schwoebel and E. J. Shipsey, J. Appl. Phys. **37**, 3682 (1966).

[38] N. A. Deskins and M. Dupuis, Phys. Rev. B **75**, 195212 (2007).